Biophysical Chemistry 6 (1977) 173–189

KINETICS OF THE POLYMERIZATION REACTION OF TOBACCO MOSAIC VIRUS PROTEIN: TRANSIENT-SATURATION TYPE POLYMERIZATION REACTION

Hideki TACHIBANA, Yuzuru HUSIMI and Akiyoshi WADA
Department of Physics, Faculty of Science, University of Tokyo, Hongo, Bunkyo-ku, Tokyo, Japan

Received 12 November 1975
Revised manuscript received 28 October 1976

The kinetics of the endothermic polymerization reaction of tobacco mosaic virus protein in the mild acid region was studied by means of temperature-jump (rising time of 6 sec)-turbidimetry, electron microscopy, and computer simulation. The time course profile of the turbidity increase changed from a normal one to an anomalous one as the size of the temperature-jump was made greater. The anomalous type polymerization profile, which we named the "transient-saturation" type, could be characterized by a rapid increase of turbidity and its transient saturation, and a slow increase to the final level. At a higher concentration of the protein, this transient-saturation effect was more marked, whereas the slow increase of turbidity in the second phase occurred with a higher rate. This transient-saturation type polymerization profile was observed also in a pH-induced polymerization reaction. It was not observed in the case of the N-bromosuccinimide modified tobacco mosaic virus protein under a similar environmental change. By an electron microscopic study and computer simulation, it was revealed that in the first phase, a large number of short polymers were formed, and the concentration of the polymerizing units was rapidly reduced to the equilibrium value, and the polymerization reaction stopped transiently. In the second phase, polymer-polymer associations took place slowly and longer polymers were formed. The relevance of the present study to the polymerization reaction of actin, myosin, and to a transient-overshoot type polymerization are discussed.

1. Introduction

It is known that separately prepared tobacco mosaic virus (TMV)-protein and TMV-RNA copolymerize, and reconstitute into a rod-like particle [1]. It has also been found that TMV-protein alone can polymerize into a rod-like particle [2]. This polymerization is favored in a slightly acidic pH region, high salt concentration, and at high temperature. Lauffer et al. first found this endothermic and reversible polymerization reaction [3], and a series of their kinetic and static experiments clarified several factors contributing to the polymerization; for instance, an increase in entropy associated with the water release from the protein during the polymerization process [4]. They determined the enthalpy and entropy changes for the polymerization reaction from osmotic pressure and turbidity measurements.

There are several works on the kinetics of the polymerization reaction of TMV-protein; in the acid pH region including the region below the isoelectric point [5], and on the 20 S disk formation reaction in the neutral or mild alkaline region [6,7]. Recent studies [8,9] have shown that an overshoot (in the average degree of polymerization) occurs after a rapid environmental change from that favoring depolymerization to that favoring polymerization.

In the present report, the kinetics of the polymerization reaction of TMV-protein in the mild acid region was studied. As the reaction is temperature sensitive, and not so rapid (from tens of seconds to hours), we used a thermal-conduction type temperature-jump method (rising time of 6 s) which had been used in the study of the denaturation-renaturation kinetics of single globular enzymes [10,11]. A new type of time course profile different from that of the overshoot type was found.

2. Materials and methods

2.1. Sample preparation

TMV, Japanese common strain OM, was purified by centrifugation fractionations in essentially the same

way as done by Boedker and Simmons [12].

TMV-protein was prepared by either the acetic acid method [13] or the alkaline method of Durham [7]. The maximum to minimum ratio of the ultraviolet absorption spectrum was more than 2.5 at pH 6.5 and 4°C. In all measurements, phosphate buffer (KH_2PO_4/Na_2HPO_4) of an ionic strength of 0.1 was used unless otherwise specified. The protein concentration was determined spectrophotometrically using the extinction coefficient of 1.27 for a 1 mg/ml solution at 282 nm [13]. It sedimented as a single peak of 3.0 S ($s_{20,w}$ value) at pH 6.5 and 4°C, when the protein concentration was lower than 2 mg/ml.

N-bromosuccinimide (NBS) modification of TMV-protein was done following the method of Ohno et al. [14]. The extinction coefficient of NBS-modified TMV-protein was taken to be 1.33 for a 1 mg/ml solution at 281 nm [15]. It sedimented as a single peak of 3.9 S at pH 6.2 and 4°C when the protein concentration was lower than 3 mg/ml.

In 0.1 M sodium pyrophosphate buffer at pH 7.2 and 25°C, after one day of equilibration, the sedimentation velocity $s_{20,w}$ of NBS-modified TMV-protein was 8 S in agreement with the results of Ohno et al. [14], whereas that of TMV-protein was 19 S and 37–38 S at the concentration of 2–4 mg/ml.

2.2. Turbidity measurement

The turbidity of the solution was measured using a Hitachi 124 spectrophotometer equiped with a thermojacket, at a wavelength of 320 nm in the case of TMV-protein, and at 340 nm in the case of NBS-modified TMV-protein.

To make sure that the apparatus gave true turbidity values, we placed a slit in front of the photomultiplier and measured the optical density of TMV solution [16]. It increased by about 4% with a slit having the diameter of 1 mm over the case without a slit, and the actual measurements were done without a slit.

The multiple scattering effect was examined using TMV solutions of various concentrations. It was shown that the decrease in the optical density due to multiple scattering was less than 2.5% for the typical turbidity values in the present experiment.

The temperature of the solution was measured by a thermistor placed in the solution, and was accurate within 0.1°C.

2.3. Temperature-jump

The temperature-jump cell used was a thermal-conduction type, and was almost the same as that described by Segawa et al. [11]. The solution was put into a thin fused-silica tube of inner diameter 2.0 mm, outer diameter 2.6 mm, and length 10 mm. Water from one of the two constant temperature circulators which were thermostated at temperatures T_1 and T_2 flowed outside the cell, and the temperature-jump was carried out by switching the flow. It took about 6 s for the completion of a temperature-jump, when judged from the absorbance change of the pH-indicator, p-Nitrophenol (p-NP). This value did not depend on the initial or final temperature employed in this experiment. The temperature of the circulating water was controlled within 0.1°C.

2.4. pH-jump

The pH-jump experiment was performed by injecting a concentrated buffer solution into the protein solution to attain the final pH and ionic strength required. The solution initially had a high pH and low ionic strength (completely depolymerized state), and was put into a 1 × 1 × 4 cm cell with a stirrer at a controlled temperature. The time for the completion of mixing was found to be shorter than 2 s as judged from the absorbance change of the p-NP solution. The ionic strength before and after a pH-jump was not the same in the present experiment.

2.5. Electron microscopy

A JEOL 100-U electron microscope was used at 80 kV with an instrumental magnification of ×20 000. The magnification was determined by reference to the 395 A period of the tropomyosin magnesium tactoids using an optical diffraction method [17]. Polystyrene-latex spheres (1090 Å average diameter) were also used.

To study the distribution of polymers after a temperature-jump, the protein solution which had been put into a very small test tube (2 mm diameter, 40 mm length) was transferred from one temperature controlled bath to another. The rising time of the temperature in the small test tube was the same as in the optical cell for temperature-jump-turbidimetry. At various times after a temperature-jump, the protein solution was sampled by a syringe equilibrated at the same

temperature, and put on a carbon-coated copper grid. Immediately it was rinsed with several drops of water at the same temperature, and then stained with several drops of the 2% solution of uranyl acetate. The excess liquid was removed with a filter paper, and the grid was allowed to dry. The process of rinsing was essential for the polymer particles to disperse well on the observation field and to avoid an additional polymerization reaction introduced by the low pH of the uranyl acetate solution [18].

To test that the specimen grid preparation showed the true distribution of polymers in the solution, the spray-shadow method was also employed. The solution was sprayed from a nebulizer to the grids, which were then shadow casted by a Pt-Pd (80:20) alloy of 15 mm length and 0.1 mm diameter with a shadowing angle of $\tan^{-1}(1/5)$.

In most cases, several hundred polymers from different mesh fields, grids, and different runs of the experiment were measured.

2.6. Optical constants and particle dissipation factors

Following Smith and Lauffer [19] an H_λ value of 4.23×10^{-5} (cm/g)^2 at a wavelength of 320 nm was used to calculate the turbidity ($\tau = H_\lambda \Sigma_i c_i M_i Q_i$) from the length distribution of polymers obtained by electron microscopy. Here H_λ is an optical constant, c_i is the concentration of protein polymers in g/ml in the ith length class, M_i is its molecular weight, and Q_i is its particle dissipation factor. And it was compared with the optically measured turbidity value. If they agree, it means that the weight fraction of the monomer protein (or oligomers), which can hardly be detected by electron microscopy, is small under the present experimental condition. The particle dissipation factors were calculated following the theoretical formula for the rod shaped particle [16].

In the case of NBS-modified TMV-protein, $H_{340\,nm}$ was calculated from $H_{320\,nm}$ for TMV-protein using the λ^{-4}-law on the assumption that both the refractive index of the solution and its increment had the same values as for TMV-protein at 320 nm.

2.7. Computer simulation

Theoretical time courses in the population change of polymers belonging to each length class, and those of the change of the weight average degree of polymerization under a given model scheme, were calculated by the numerical integration of a set of ordinary differential equations describing the reaction kinetics.

The Runge-Kutta-Gill, or Euler method [20] was used for the calculations which were done using the HITAC 8800/8700 system at the Computer Center of Univ. of Tokyo. The former method was employed where precision was needed, and the latter where the speed of the calculation was needed. In all cases, the value of the smallest population of the polymers changed only in the third of fourth decimal place, when the discretization width for the numerical integration was reduced by 1/10. Care was taken to avoid the round-off error, and the double precision calculation only resulted in changing the final integrated value of the smallest population of the polymers at the third or fourth decimal place.

3. Results

3.1. Turbidimetry

3.1.1. Static experiments

The endothermic and reversible polymerization reaction of TMV-protein, and NBS-modified TMV-protein are shown in fig. 1. They occur at higher temperatures as the pH is made higher, and the maximum turbidity is smaller in the higher pH region. At pH 6.5, TMV-protein is in the depolymerized state at low temperatures, and in the polymerized state at room temperature.

These features are in agreement with the results of Smith and Lauffer [19], and Shalaby and Lauffer [21] except that the temperature range for polymerization is about 4–5°C lower in the present case. This does not seem to come from the difference in the protein concentration used (1 mg/ml in the present experiment, and 0.88 mg/ml in the Smith and Lauffer experiment). As there is no difference in the method of preparation of the protein or the equilibration time at each temperature, the difference in the temperature range may be attributable to the difference in the nature of the protein between *Vulgare* strain and Japanese common strain OM; there are two alterations in the amino acid sequence from one to the other protein [22].

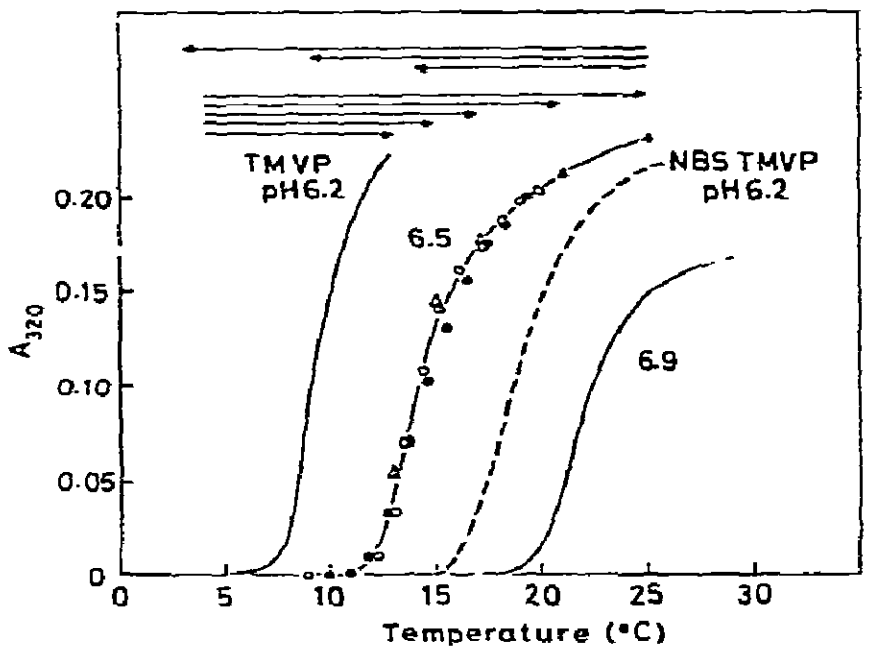

Fig. 1. Turbidity increase and decrease due to the polymerization and depolymerization reactions of TMV-protein (——) and NBS-modified TMV-protein (– – –) as a function of temperature. In this figure and the following ones, turbidity, τ, is given as absorbance, A, in the ordinate; $\tau = 2.303A$. Protein concentration is 1.0 mg/ml and pH values at 25°C are given. Final values under very slow (rising time of several minutes), stepwise temperature increases (○), decreases (●), and that under temperature-jumps (△) as in fig. 2 are shown at pH 6.5. The full or broken lines are the averages of several experimental values. In the case of NBS-modified TMV-protein, the values for A_{320nm} were calculated from these for A_{340nm} using λ^{-4} law. The arrows cover the initial and final temperatures of the various temperature-jumps at pH 6.5, the results of which are shown in fig. 2 and fig. 5.

NBS-modified TMV-protein can also polymerize endothermically and reversibly in the mild acid region [15], but the temperature range for polymerization is about 8°C higher than that for TMV-protein. In other words, in the same temperature range, it polymerizes at a lower pH than TMV-protein. It is known that NBS-modified TMV-protein cannot make a 20 S disk structure under the condition for the reconstitution experiment [14,15]; this was also true in the present experiment as described in section 2.1. This fact is due to the extra minus charge of dibromotyrosine at the amino acid residue 139. The above mentioned difference in the polymerization reaction in the mild acid region can also be explained by this extra minus charge.

A kinetic experiment was carried out by temperature-jumps which are indicated by the arrows shown in fig. 1. At pH 6.5, the initial temperature was set at 4°C. There, the dominant component of the protein is a trimer as has been known [3,4,19,21] and as shown by the results of the sedimentation velocity experiment described in section 2.1.

For the interpretation and simulation of the kinetic time courses, which will be shown later, it is necessary to know the value of the equilibrium constant for the polymerization reaction, K, at the final temperature. As was derived by Smith and Lauffer [19], K is given by $[(\tau/\tau_0)^2 - 1]/4c_0$ in a linear condensation model. Here, τ is the turbidity, τ_0 is the initial turbidity of the trimer solution, and c_0 is the initial molar concentration of the trimer. In the temperature range where the polymerization reaction begins to be observed, $\tau \gtrsim \tau_0$, and K is of the order of c_0^{-1}; in the present case it is about 10^5 M^{-1}. In the temperature range where the optical density exceeds 0.2 (20–25°C), K is of the order of 10^{8-9} M^{-1}. More precise values of K cannot be obtained in this way, for the assumptions used to derive the above formula are not fully satisfied.

3.1.2. Time course of polymerization

The time courses of the polymerization of TMV-protein at pH 6.5 after various temperature-jumps are shown in fig. 2. An interesting fact is that the time course profile changes to an anomalous type in the cases having high final temperatures of 21 and 25°C. In these cases the time course profile can be characterized as follows; at first, there is a rapid burst of the turbidity increase and an abrupt stoppage at about half the level of the final turbidity, and second, it

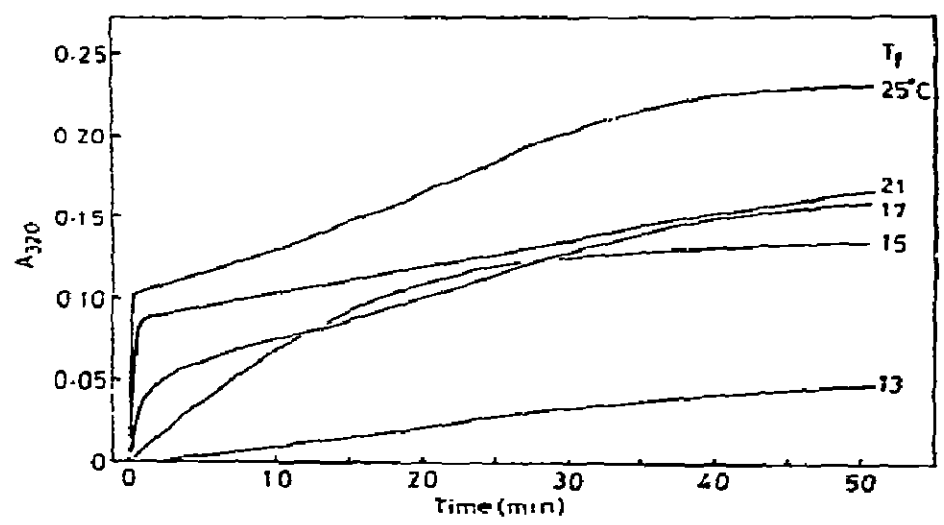

Fig. 2. Polymerization time course of TMV-protein (1.0 mg/ml) at pH 6.5, for various temperature-jumps. The initial temperatures are 4°C for all cases, and the final temperatures, T_f, are shown in the figure.

passes through an inflection point, then slowly increases until it ultimately reaches the final value. The final level agrees with that obtained by the static experiment. In short, this complex time course profile can be divided into two phases; the transient-saturation phase and the slow increase phase.

The quantities associated with this transient-saturation type polymerization profile, e.g., the turbidity where the transient-saturation occurred and the rate of the turbidity increase in the second phase, varied within 30% from one sample preparation to another. However, their qualitative features as described above were always the same.

This transient-saturation type polymerization was also observed at pH 6.9 as shown in fig. 3. In this case the overall polymerization reaction occurred more rapidly than at pH 6.5, and the inflection was not marked.

The concentration dependence of the profile of the transient-saturation type polymerization is shown in fig. 4. The results are summarized as follows. First, the turbidity value normalized to the protein concentration at the point where the transient-saturation occurs decreases with increasing concentration. Second, the rate of increase in turbidity in the second phase increases with the concentration, and is approximately proportional to the second power of the concentration.

3.1.3. Time course of depolymerization

When we study the mechanisms which produce the

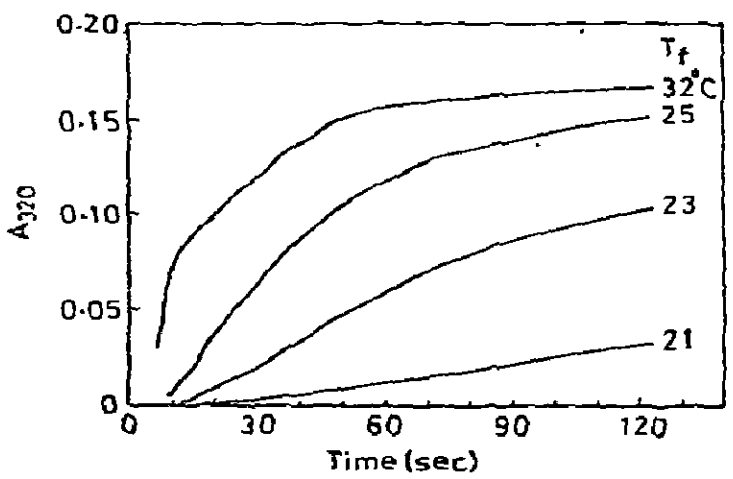

Fig. 3. Polymerization time courses of TMV-protein (1.0 mg/ml) at pH 6.9, for various temperature-jumps. The initial temperatures are 11°C for all cases, and the final temperatures, T_f, are shown in the figure.

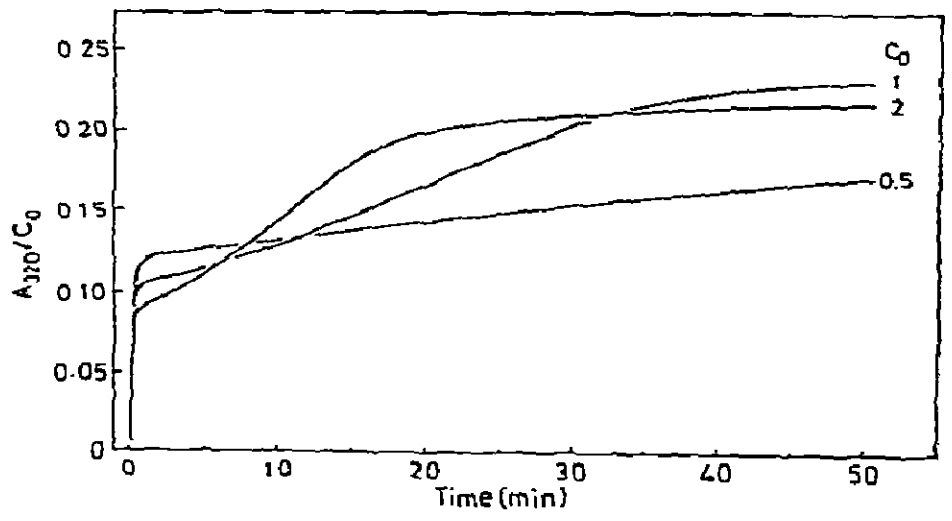

Fig. 4. Concentration dependence of the polymerization time course of TMV-protein at pH 6.5, for a temperature-jump from 4 to 25°C. Protein concentrations, c_0, are 2.0, 1.0, and 0.5 mg/ml. The ordinate is normalized to the concentration, and is proportional to the weight averaged molecular weight of polymers reduced by the particle dissipation factors. The initial rates in the second phase are 0.104, 0.030, and 0.007 A_{320}/10 min for c_0 = 2.0, 1.0, and 0.5 mg/ml respectively. These are approximately proportional to the second power of c_0.

transient-saturation type polymerization profile, we must first know the order of the magnitude of the depolymerization rate constant. The time courses of the depolymerization after the temperature-jumps to lower temperatures, which are indicated by the arrows in fig. 1, are shown in fig. 5 (a). The results show that the initial depolymerization rate is higher in the case of lower final temperatures. As shown in the appendix, the initial rate of the turbidity decrease is proportional to the rate of depolymerization, k_4.

The temperature dependence of k_4 is shown in fig. 5 (b). The apparent activation enthalpy is negative, and -19.1 ± 1.4 kcal/mol. The appearance of a negative activation enthalpy is also seen in the case of the depolymerization reaction of tubulin [23].

It is necessary to use a well-defined initial state of polymerization in the experiment of the depolymerization reaction. The distribution of the polymer length depends on the temperature, the equilibration time at that temperature, and the velocity of the temperature increase from the depolymerized state to the polymerized state. The initial state of polymerization for the present experiment is attained 60 min after a temperature-jump from 4 to 25°C. The distribution of polymers in this state was examined by electron

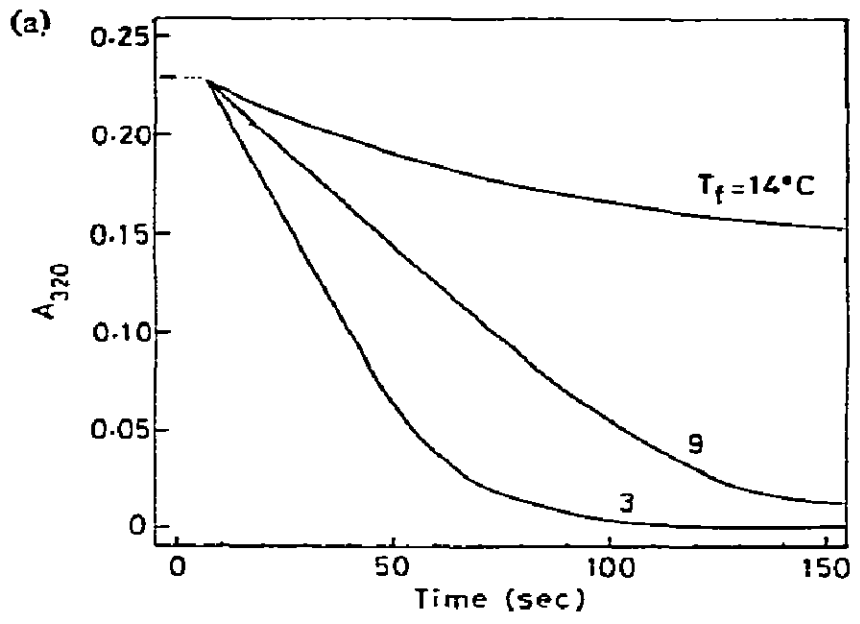

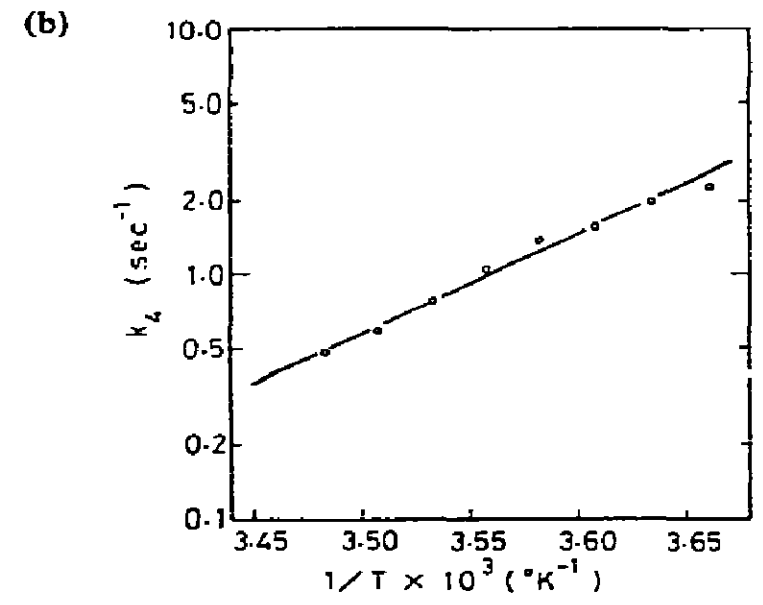

Fig. 5. (a) Depolymerization time courses of TMV-protein (1.0 mg/ml) at pH 6.5, for temperature-jumps from 25°C to various final temperatures, T_f, indicated in the figure. (b) Arrhenius plots of the apparent depolymerization rate constants calculated from the initial slopes of such curves as shown in (a).

microscopy and the result will be shown in fig. 9 (a). There the lengths of the polymers are comparable with the wavelength of the light for the turbidity measurement; it was calculated that the weight average degree of polymerization obtained from the observed turbidity value was about 55% of the true value due to the particle dissipation.

Taking into account this correction, the rate constant of the depolymerization at 25°C can be estimated (by extrapolation of the k_4 vs. temperature relation) to be about 0.3 s^{-1} for the depolymerizing unit of the trimer. The equilibrium constant, K, is of the order of 10^{8-9} M^{-1} at 25°C as previously shown. Consequently, the rate constant of polymerization, k_3, can be estimated to be of the order of 10^{7-8} M^{-1} s^{-1} at 25°C and pH 6.5.

3.1.4. Polymerization time course of NBS-modified TMV-protein

NBS-modified TMV-protein cannot make a 20 S disk structure at pH 7.2 and cannot initiate the reconstitution reaction with TMV-RNA, whereas it can elongate the partially reconstituted helical rod [14]. In the mild acid region as in the present experiment, the phenol group of dibromotyrosine in NBS-modified TMV-protein still dissociates partially. So, if the disk structure (or the structure related with it) participates in the nucleation of the TMV-protein polymerization reaction, it may be expected that the time course profiles of the polymerization after a temperature-jump are different for NBS-modified TMV-protein and the unmodified TMV-protein.

The time courses of the polymerization of the NBS-modified TMV-protein after various temperature-jumps are shown in fig. 6 (a). The marked difference from that of TMV-protein is the absence of the transient-saturation type profile even if the final temperature is high enough. This point is also true at different concentrations of the protein as shown in fig. 6 (b). The characteristic dependence of the transient-saturation type polymerization profile on the concentration has not been observed.

The depolymerization rate constant, k_4, which had also a negative activation enthalpy of about −29 kcal/mol, was found to be of the order of 10^{-1} s^{-1} at 30°C. The rate of the polymerization, k_3, estimated in the same way as in TMV-protein, is also of the order of 10^{7-8} M^{-1} s^{-1}. So, as far as this point is concerned the situation is similar to that in TMV-protein. Thus it seems that the difference in the profiles is most probably due to the difference in the nucleation reactions.

3.1.5. pH-jump experiment

The polymerization reaction of TMV-protein can also be induced by a pH change from the alkaline to the slightly acidic region, at a constant temperature. The fact that the transient-saturation type polymerization does occur in the pH-induced polymerization is shown in fig. 7. At a lower temperature, the time course profile is a normal one. Thus, the transient-saturation type polymerization is a general phenom-

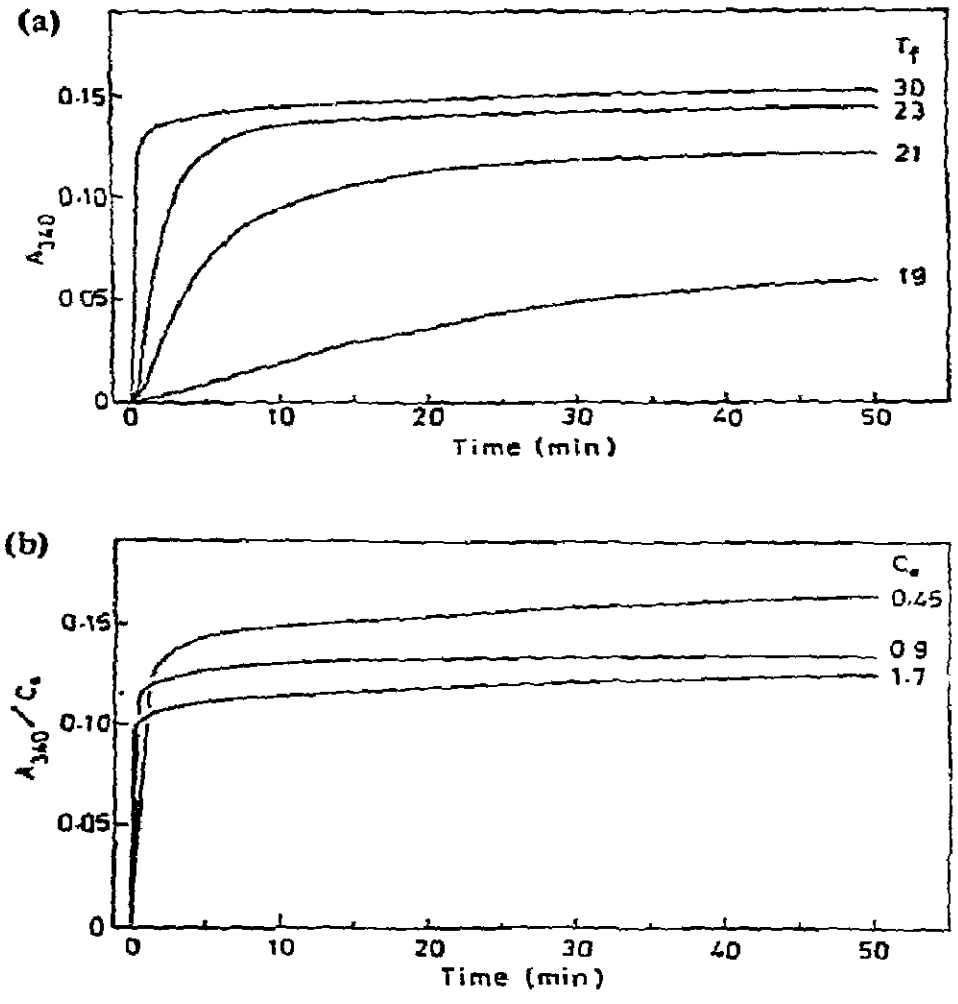

Fig. 6. (a) Polymerization time courses of NBS-modified TMV-protein (0.9 mg/ml) at pH 6.2, for various temperature-jumps. The initial temperatures are 9°C for all cases, and the final temperatures, T_f, are shown in the figure. (b) Concentration dependence of the polymerization time course of NBS-modified TMV-protein at pH 6.2 for a temperature-jump from 9 to 30°C. Protein concentrations, c_0, are 1.7, 0.9, and 0.45 mg/ml. The ordinate is normalized to the concentration. The sample batch is different from that used for the curves in (a).

enon associated with a rapid and large jump of external parameters from a depolymerized state to a highly polymerized state.

In the pH-jump experiment the overall reaction is more rapid than in the temperature-jump experiment, though the final condition is the same. Moreover, the final turbidity reached is lower. The difference in the state of the protein in the initial state (pH 7.5, ionic strength 0.002, and at 25°C in the pH-jump, whereas pH 6.5, ionic strength 0.1, and at 4°C in the temperature-jump) may be involved here, though the protein is completely depolymerized below the level of the trimer in both cases.

The protein brought to a pH level of 6.5 in the pH-jump experiment had the same nature once its temperature was brought to 4°C as that prepared at pH 6.5 and at a constant temperature of 4°C; the former protein showed a typical transient-saturation type polymerization profile as well as the latter one for the temperature-jump from 4 to 25°C at pH 6.5 as shown in fig. 2.

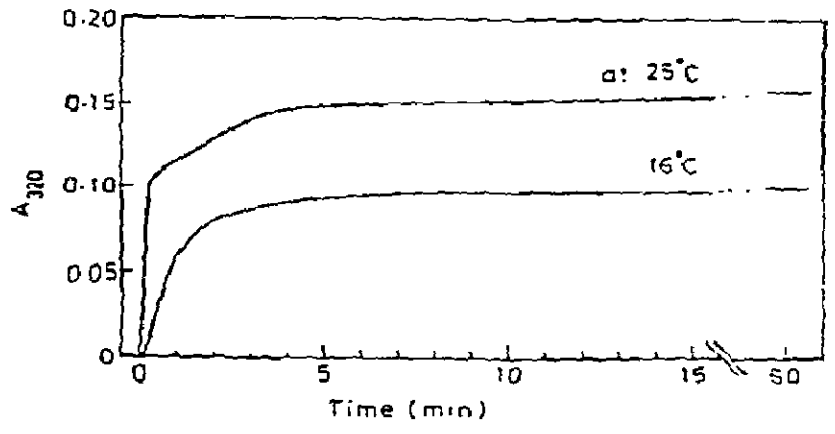

Fig. 7. Polymerization time courses of TMV-protein for a pH-jump. The conditions of the initial solution were: TMV-protein 1.2 mg/ml, ionic strength 0.002, pH 7.5 and at the controlled temperature indicated in the figure. To this, phosphate buffer with a volume 1/5 that of the initial solution and with an ionic strength of 0.6, was added to reach the final conditions: TMV-protein 1.0 mg/ml, ionic strength 0.1 and pH 6.5.

3.2. Electron microscopy

3.2.1. Comparison of the sample grid preparation methods

Turbidity reflects the weight average molecular weight of the polymers corrected for the particle dissipation factors. But it cannot be used to describe the precise distribution pattern of the molecular weight, e.g., whether it is a single-peak distribution or two-peak one. As a result, we examined by electron microscopy the distribution of the polymers after a temperature-jump.

In spite of the advantage of obtaining a distribution of polymers, there are disadvantages in electron microscopy that samples must be dried, and stained or shadowed. The fact that short or long polymers are not selectively adsorbed or detached from the grid surface under the rinsing process, and that the length of the polymers do not change under an acidic condition of the staining solution, was tested as follows.

It was found that a large number of very short

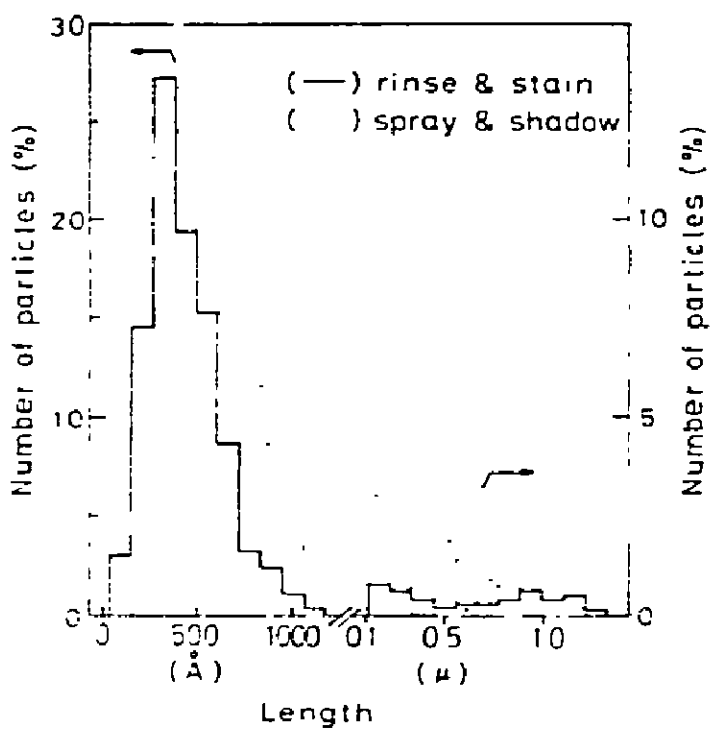

Fig. 8. Length distribution of TMV-protein particles obtained by the two different electron microscope grid preparation methods. The TMV-protein solution (1.0 mg/ml) at pH 6.5, was very slowly (rising time of several minutes) warmed from 4 to 25°C. After about 25 min, one part of the solution was applied to the electro microscope grid, rinsed and stained (full line). The other part was sprayed by a nebulizer and shadowed (dotted line). The lengths were measured in steps of 110 Å for shorter particles (left part of the figure), and 1100 Å for longer particles (right part). The total number of the particles measured was 932 for rinse-stain method, and 428 for spray-shadow method.

polymers and a small number of long polymers were formed when the temperature of the TMV-protein solution was very slowly (rising time of several minutes) raised from 4 to 25°C. This state of polymer distribution was examined by two different ways in preparing the electron microscope sample grid. The results are shown in fig. 8. One is a rinse-stain method, and the other is a spray-shadow method. In the latter method there are two advantages. First, all the particles present in the solution are transferred and preserved on the grid. Second, as the diameter of the solution droplet sprayed from a nebulizer onto the grid is very small (1—20 μ, directly observable in the electron microscope image field) and the droplets of these diameters dry rapidly (about 0.1 s), the change of the particle length due to additional reactions is small [24].

On the other hand, there are also some difficulties in this spray-shadow method. First, phosphate buffer, not being volatile, was deposited, and made it difficult to measure the lengths of the polymers among it. The dilution of the sample solution with a volatile buffer before spraying is not suitable for the concentration dependent and reversible reaction system as in the present case. Second, the lengths of the particles were measured to be long as compared with those prepared by the rinse-stain method, perhaps because of the granularity and the piling-up effect of the shadowing material. Third, in the concentration range used in this study, the density of the particles, as sprayed down to the grid, was too high and particles were not so well dispersed.

The results in fig. 8 show that as far as relatively short particles are concerned the preservation of the polymer distribution in the rinse-stain method is rather good considering the effect of the increase in the particle size in the spray-shadow method. We used the rinse-stain method in the present study.

3.2.2. The change in polymer distribution

One set of electron micrographs of TMV-protein polymers formed during the time course of the transient-saturation type polymerization is shown in fig. 9. From this and many similar ones the length distribution of the polymers is obtained and shown in fig. 10 (a). At the time when the transient-saturation occurs (about 20 s), a large number of short polymers having a narrow peaked distribution is formed. The weight average length is 710 Å, and is about 47% of that at 60 min (1520 Å). In the middle of the second phase (10 min), the distribution is shifted toward the longer length region. At 60 min after the temperature-jump, a broad peaked distribution centered at a length of about 1300—1400 Å is attained.

In the case of NBS-modified TMV-protein, the above characteristics for TMV-protein is less marked as shown in fig. 10 (b). First, at 20 s after the temperature-jump, longer particles are formed than in the case of TMV-protein, and the distribution is more broad. Second, the shift of the distribution to the longer length region at 10 min is less marked. After 60 min, longer particles are formed than in the case of TMV-protein.

Thus, TMV-protein under the temperature-jump from 4 to 25°C produces many short polymers at first, and then longer polymers are formed. This is a clear contrast to the situation in the overshoot polymerization, and shows that nucleation is easy in the transient-saturation type polymerization. On the

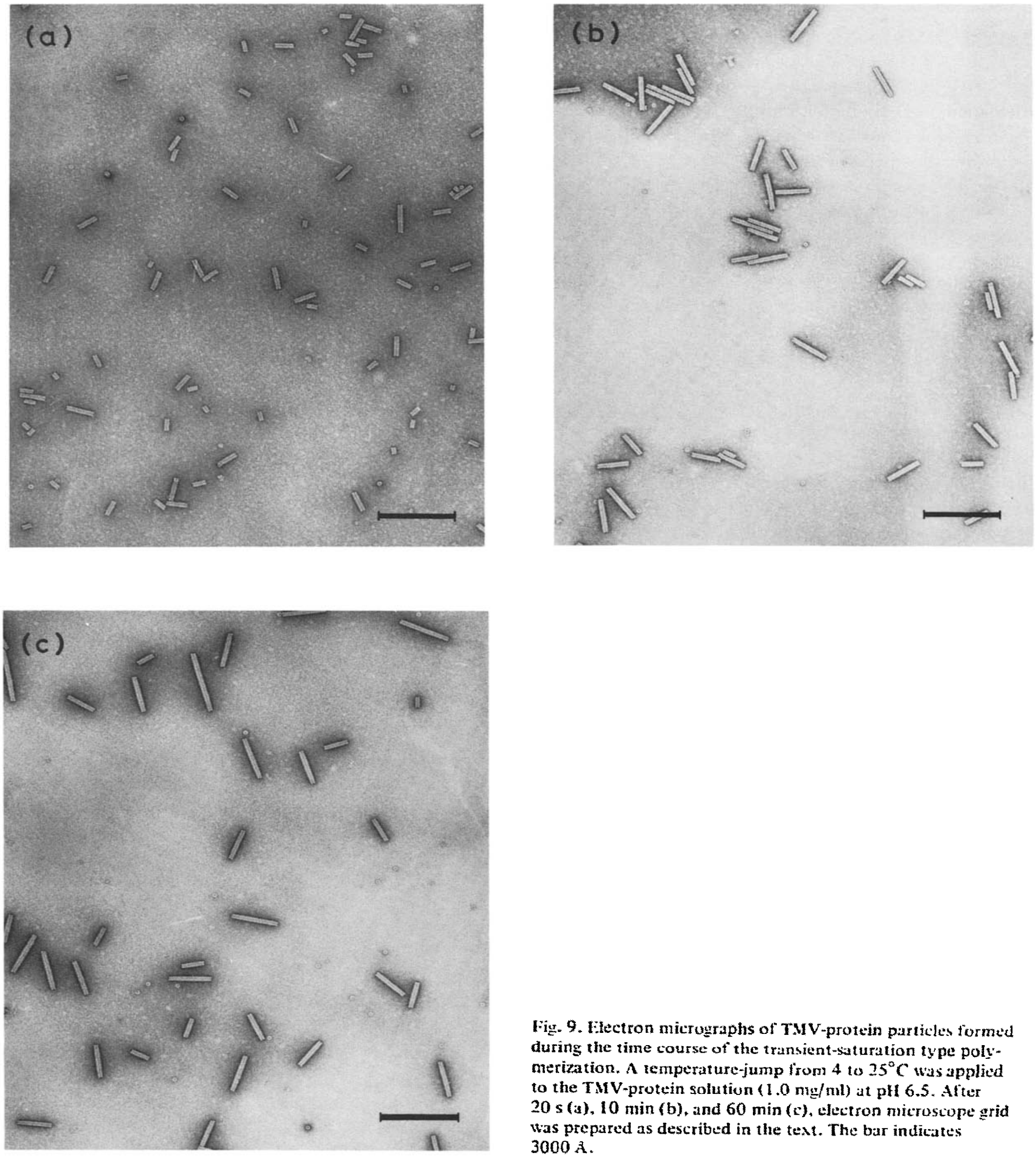

Fig. 9. Electron micrographs of TMV-protein particles formed during the time course of the transient-saturation type polymerization. A temperature-jump from 4 to 25°C was applied to the TMV-protein solution (1.0 mg/ml) at pH 6.5. After 20 s (a), 10 min (b), and 60 min (c), electron microscope grid was prepared as described in the text. The bar indicates 3000 Å.

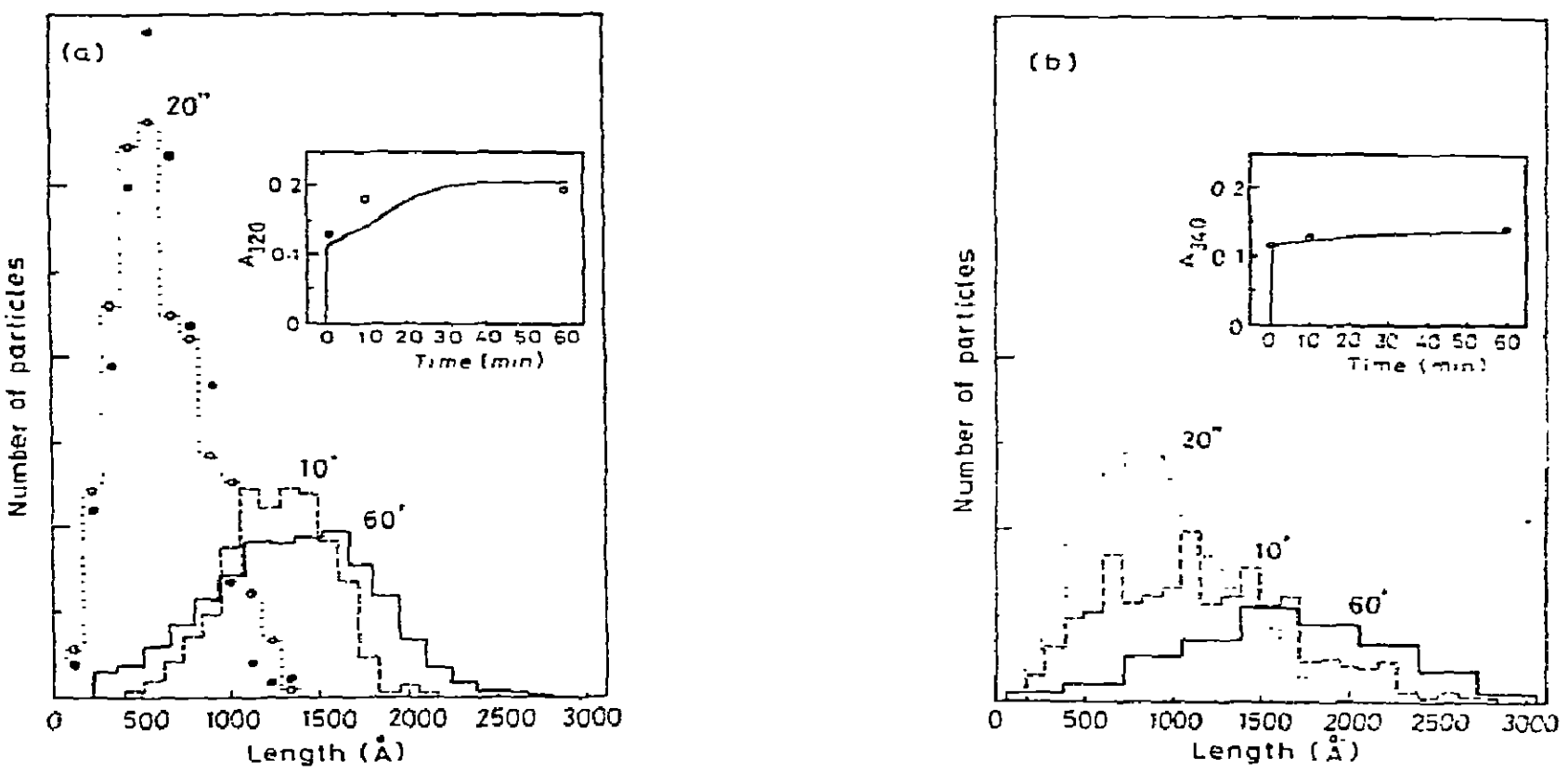

Fig. 10. (a) Length distribution of particles of TMV-protein (1 mg/ml) after a temperature-jump from 4 to 25°C at pH 6.5. Lengths were measured in steps of 110 Å for the distribution at 20 s (·····) and 10 min (– – –), and 145 Å for that at 60 min (——). The ordinate is normalized in such a way that $\Sigma\, in_i$ is equal for all three distributions, where i specifies the length class, and n_i is the number of particles in the ith class (including the corrections due to the difference in the class width). At 20 s, two distinct distributions obtained by the same procedures, but using different batches of proteins, are shown; (○) and (●). Total numbers of particles measured were 393 (○), 459 (●), 424 (– – –), and 892 (- ——). Inset: Time course of the spectrophotometrically measured turbidity increase under the temperature-jump (——), and the turbidity values calculated from the length distributions in this figure (○). (b) Length distribution of particles of NBS-modified TMV-protein (0.9 mg/ml) at pH 6.2 after a temperature-jump from 9 to 30°C. Other details are the same as in (a). For the distribution at 60 min, lengths were measured in steps of 330 Å. Total numbers of particles measured were 853 (·····), 374 (– – –), and 221 (——). The inset is the same as in (a).

other hand the fact that NBS-modified TMV-protein produces longer polymers than in the case of TMV-protein can be explained by its difficulty in nucleation. But it was kinetically not so slow as to give the overshoot type polymerization.

These results are based on the distribution data of side-on polymers. As shown in fig. 9, an end-on setting of polymers is frequently observed among side-on polymers. The number fraction of the end-on polymers are about 30%. To know their heights, negatively stained grids were further shadow casted. The results showed that the mean height was below 100 Å. End-on polymers with nearly the same length of shadows as side-on polymers were only rarely found. From this fact, the weight fraction of the end-on polymers can be estimated to be below 3%.

3.3. Computer simulation

3.3.1. Reaction scheme

We consider the addition polymerization scheme containing three distinct reaction steps; nucleation, elongation, and termitation as follows:

$$\text{Nucleation:} \quad 2\text{M} \underset{k_2}{\overset{k_1}{\rightleftharpoons}} \text{P}_2$$

$$\text{Elongation:} \quad \text{P}_i + \text{M} \underset{k_4}{\overset{k_3}{\rightleftharpoons}} \text{P}_{i+1} \qquad (2 \leqslant i < 9)$$

$$\text{Termination:} \quad \text{P}_9 + \text{M} \underset{k_4}{\overset{k_3}{\rightleftharpoons}} \text{P}_{10}\,.$$

Here, the nucleus is composed of 2 monomers, and k_1 and k_2 are its formation and dissociation rate con-

stants, respectively; k_3 and k_4 have the same meaning as defined in section 3.1.3. Further we define $K_n = k_1/k_2$ and $K = k_3/k_4$ as the equilibrium constants for nucleation and elongation, respectively.

In an actual TMV-protein system, the maximum length of the polymer is not definite. Mainly because of the long computing time involved, we took the degree of polymerization of the largest polymer to be 10, and that of the nucleus to be 2. This ten-component polymerization system is very small in size as compared with an actual TMV-protein system, but the essential features characteristic of a system which contains nucleation and monomer-addition reactions will be observed with this simulation system.

3.3.2. Statics

The equilibrium value of the weight average degree of polymerization, $\langle M\rangle_w$, as a function of K, with the parameter K_n, is shown in fig. 11. When the nucleation reaction is difficult ($K_n = 0.6\,K$), the polymerization reaction begins at a higher value of K than in easy nucleation ($K_n = K$). At a still higher value of K, $\langle M\rangle_w$ is greater in the case of difficult nucleation than in easy nucleation. The former phenomenon is a natural result which has already been shown theoretically [26], but the latter appears to be due to the limitation on the maximum length of the polymer. By examining the equilibrium population of each polymer at higher values of K it is seen that when nucleation is difficult, at the expense of a poor population of nuclei and short polymers, long polymers are formed more than when nucleation is easy. Because the contribution of the long polymers to the weight average molecular weight is dominant, it becomes greater when nucleation is difficult.

3.3.3. Kinetics

The time courses of the increase of $\langle M\rangle_w$ under the jump of the value of K with different degrees of ease of nucleation are shown in fig. 12 (a), (b), and (c). In an actual TMV-protein system with a temperature change from 4 to 25°C, k_3 changes greatly in magnitude from about 10^0 to 10^{7-8} M^{-1} s^{-1}, whereas k_4 changes a little from about 10^0 to 10^{-1} s^{-1}. In the simulation, k_4 is taken to be constant, 1 s^{-1}, and k_3, which is then equal to the equilibrium constant K, is taken to vary from 10^0 to 10^{5-8} M^{-1} s^{-1}.

In the case when nucleation is easy ($k_1 = k_3$,

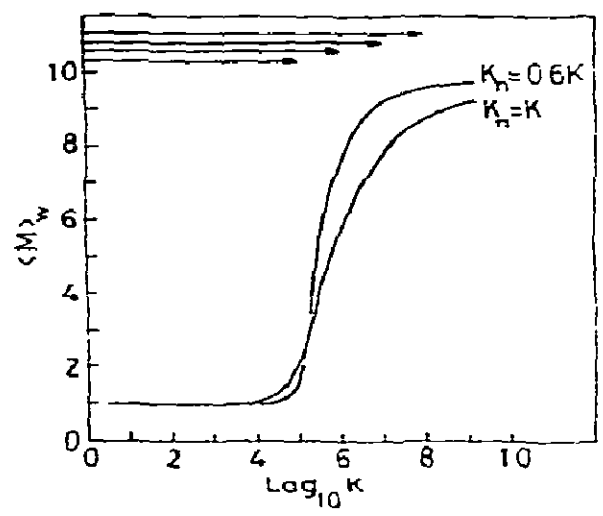

Fig. 11. Calculated curves showing the weight average degree of polymerization, $\langle M\rangle_w$, as a function of the logarithm of the equilibrium constant for polymerization, $\log_{10}K$ ($= \log_{10}(k_3/k_4)$), in a 10-component system. Two cases with different equilibrium constants for nucleation, K_n, are shown. The concentration of the monomers, c_0, is 10^{-5} M. The abscissa has approximately a linear relation with temperature, if the temperature range is small, and corresponds to the temperature axis in fig. 1. The arrows point to the final states for the jumps in the value of K. In the initial state, only monomers are present. The time courses of the increases of $\langle M\rangle_w$ for these jumps are shown in the following figures.

fig. 12 (a)), the time course profile comes to be composed of two phases as the final value of K becomes greater. The first phase is a rapid increase of $\langle M\rangle_w$, and it suddenly stops at a value of $\langle M\rangle_w$ considerably lower than that at the equilibrium. The second phase is a slow increase to the final equilibrium value. On the other hand, when nucleation is difficult as compared with elongation ($k_1 = 0.6\,k_3$, fig. 12 (b)), the change of the time course profile to the two phase type was not observed. Irrespective of the final value of k_3, $\langle M\rangle_w$ increases smoothly to the final equilibrium value.

Next, as shown in fig. 12 (c), when k_1 is varied from high to low value with k_3 left at a constant value, two types of the time course profiles of $\langle M\rangle_w$ increases are obtained; the transient-saturation type when nucleation is easy and the transient-overshoot type when nucleation is difficult.

Nucleation becomes difficult also when the dissociation of the nucleus is easy, as in the case of the polymerization reaction of actin [25]. Further simulations changing the value of k_2 as compared with k_4, and leaving the value of k_1 equal to k_3, have also been performed. The disappearance of the transient-

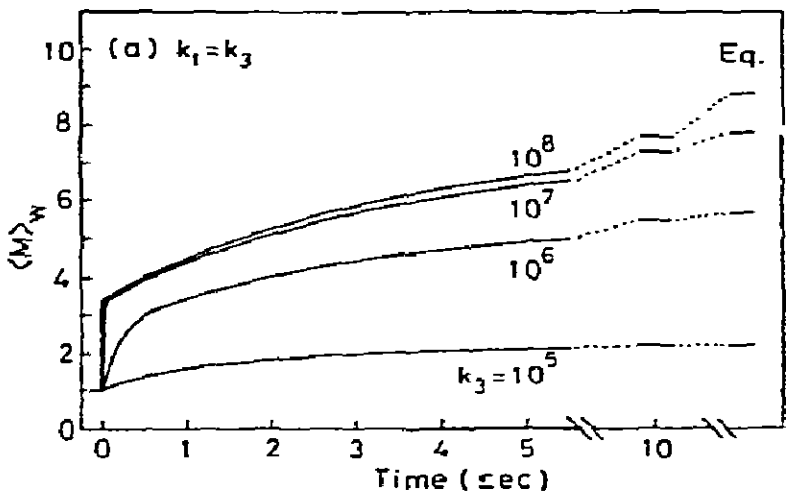

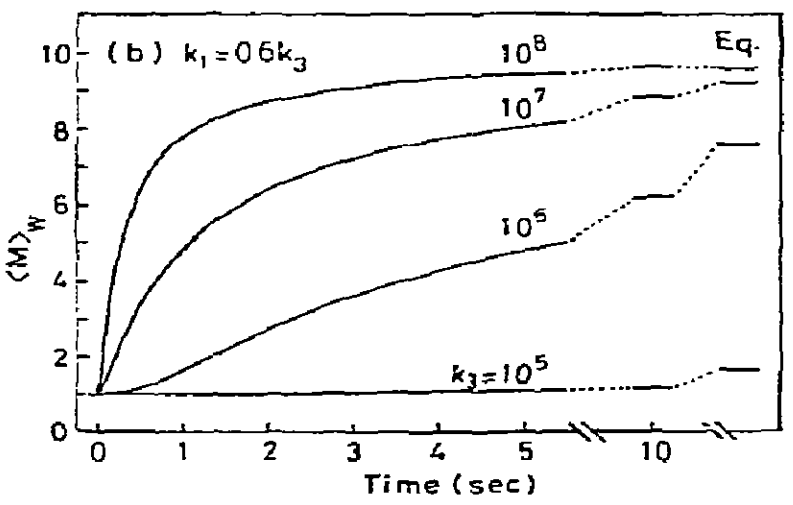

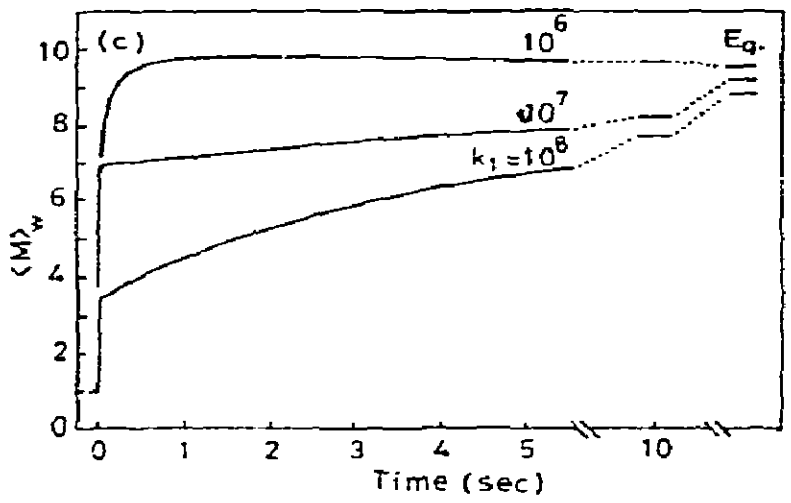

Fig. 12. (a) Calculated time courses of the increase of $\langle M\rangle_w$ in the case of easy nucleation. k_1 and k_3 are equal, and have values 10^5, 10^6, 10^7 and 10^8 M^{-1} s^{-1}. k_2 and k_4 are both equal to 1 s^{-1}. $c_0 = 10^{-5}$ M. When $k_1 = k_3 = 10^8$ M^{-1} s^{-1}, $\langle M\rangle_w$ transiently saturates with a value of 3.43 at $t = 0.01$ s, whereas the equilibrium value ("Eq." in the figure) is 8.79. The time axis cannot be compared directly with that in fig. 2 or others, because of the small size of the polymerization system for the simulation. (b) Calculated time courses of the increase of $\langle M\rangle_w$ in the case of difficult nucleation. Rate constants: $k_3 = 10^5$, 10^6, 10^7, 10^8 M^{-1} s^{-1}, $k_1 = 0.6\,k_3$ in all cases, and $k_2 = k_4 = 1$ s^{-1}; $c_0 = 10^{-5}$ M. (c) The change of the time course profile of $\langle M\rangle_w$ accompanying the change in the difficulty of the nucleation reaction. Rate constants: $k_3 = 10^8$ M^{-1} s^{-1} throughout, $k_1 = 10^6$, 10^7, 10^8 M^{-1} s^{-1}, and $k_2 = k_4 = 1$ s^{-1}; $c_0 = 10^{-5}$ M. Transient-saturation type polymerization profile ($k_1 = 10^8$ M^{-1} s^{-1}) is the same as in (a); in the case when $k_1 = 10^6$ M^{-1} s^{-1}, transient-overshoot maximum in $\langle M\rangle_w$ occurs at $t = 1.50$ s with the value of 9.80, whereas the equilibrium value is 9.46.

saturation and the appearance of the transient-overshoot were also shown as k_2 was made greater.

3.3.4. Population change in the polymerization reaction

The mechanism which causes the above mentioned two types of polymerization profiles can be understood by examining the population changes of the monomers and polymers as shown in fig. 13. First, when the transient-saturation occurs (fig. 13 (a)), the population of the monomers decreases rapidly and moreover undershoots slightly below its equilibrium value, and a peaked distribution of short polymers is formed. Afterwards, accompanying the slow increase of $\langle M\rangle_w$ in the second phase, a peaked distribution of short polymers diffuses into an exponential type distribution, producing long polymers. And the population of the monomers remains almost constant at the equilibrium value. *Second, when the transient-overshoot occurs* (fig. 13 (b)), the population of the monomers monotonously decreases to the equilibrium value, whereas the population of the longest polymers transiently overshoots slightly above the equilibrium value and causes the overshoot-maximum in $\langle M\rangle_w$. Here, it must be pointed out that this overshoot may be produced by the boundary condition of the present simulation that the maximum length of the polymer is set to be finite. An important point is the fact that once a polymer is formed, it grows into a longer one, and does not stop growing at a short length.

3.3.5. Polymer-polymer association reaction

As described above, the addition-polymerization scheme can explain the mechanism which causes the transient-saturation in the increase of $\langle M\rangle_w$. But it turned out that under the scheme, the time courses

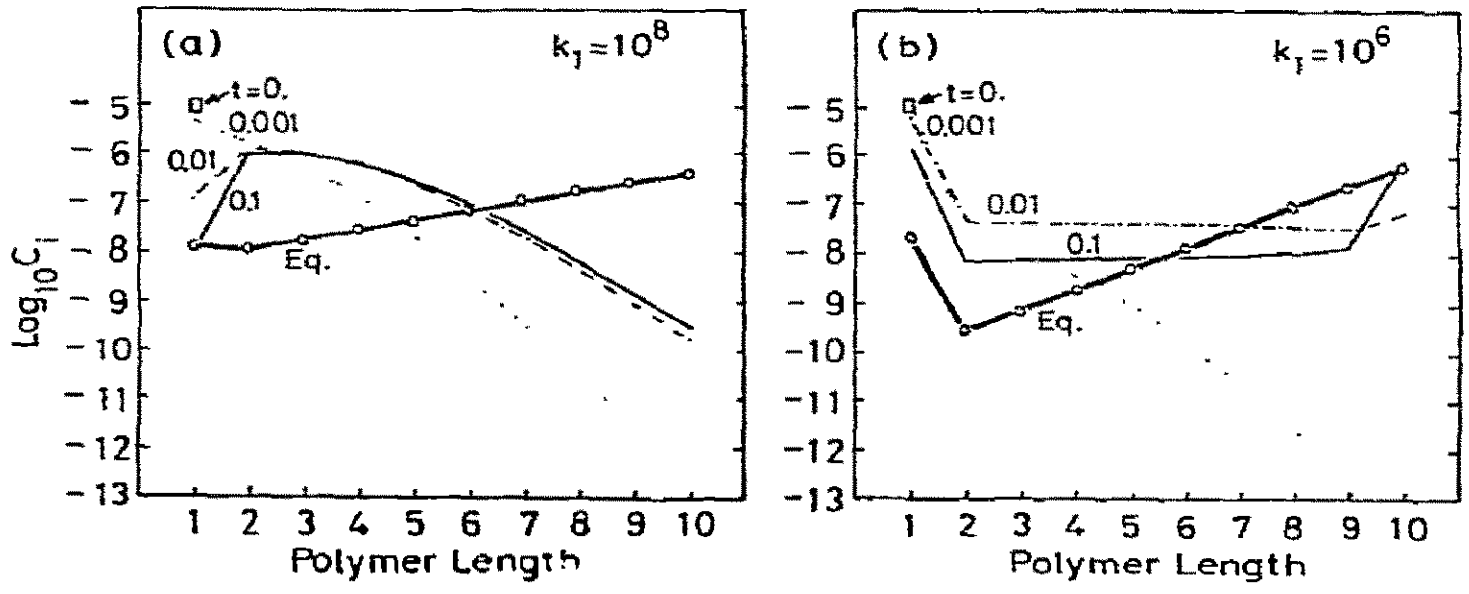

Fig. 13. Calculated changes in populations of polymers in the time courses of polymerization reactions in two cases shown in fig. 12 (c). The ordinate is the logarithm of the population of polymers. The parameter, t, is the time after the start of reaction. At $t = 0$, only monomers are present, and $c_1 = 10^{-5}$ M. (a): transient-saturation type; $k_1 = 10^8$ M^{-1} s^{-1}. The population of monomers, c_1, becomes smaller than that at equilibrium at $t = 0.023$ s and reaches a transient-undershoot minimum at $t = 3.2$ s with a value of 1.11×10^{-8} ($c_{1,eq.} = 1.56 \times 10^{-8}$). (b): transient-overshoot type; $k_1 = 10^6$ M^{-1} s^{-1}. The population of 10-mer reaches a transient-overshoot maximum with a value of 9.34×10^{-7} at $t = 0.625$ s ($c_{10,eq.} = 6.52 \times 10^{-7}$).

of the increase of $\langle M \rangle_w$ in the second phase for various protein concentrations were nearly the same, and the experimentally observed concentration dependence which is shown in fig. 4 could not be simulated.

The initial rate of the turbidity increase in the second phase is approximately proportional to the second power of the protein concentration. It is also proportional to the second power of the number concentration of the polymers formed at the time of the transient-saturation, if the average degrees of polymerization for different protein concentration are nearly equal at that time. This fact suggests that polymer–polymer-association reactions take place in the second phase.

A simulation of the time courses of the increase of $\langle M \rangle_w$ at various initial monomer concentrations when polymer-polymer association reactions are included is shown in fig. 14. To the reaction scheme in section 3.3.1. the following one is added:

$$P_i + P_j \underset{k_6}{\overset{k_5}{\rightleftharpoons}} P_{i+j} \qquad i,j \geqslant 2, \qquad i+j \leqslant 10 .$$

The results show the expected dependence of the initial slope in the second phase on c_0.

The differences between the experimental results and that of the simulation are the following two points. First, as previously described in section 3.1.2.,

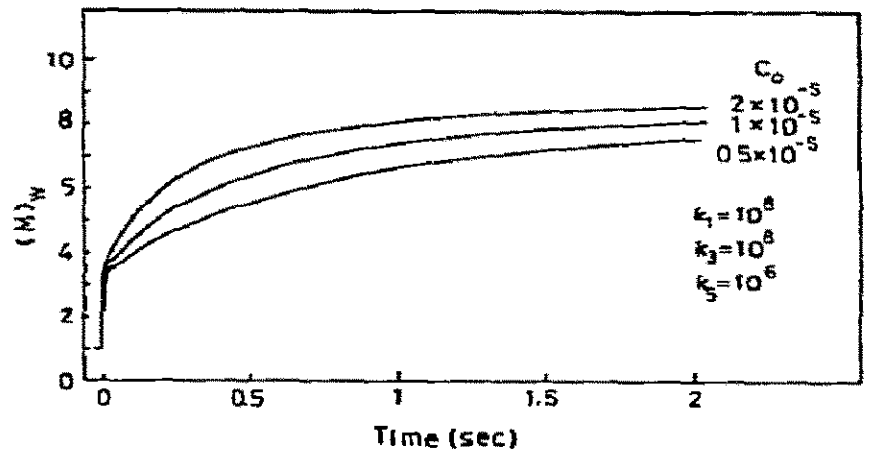

Fig. 14. Calculated time courses of the increase of $\langle M \rangle_w$ at various concentrations ($c_0 = 2 \times 10^{-5}$, 1×10^{-5} and 0.5×10^{-5} M) when polymer–polymer association reactions are included. Rate constants: in all cases, $k_1 = k_3 = 10^8$ M^{-1} s^{-1}, $k_2 = k_4 = 1$ s^{-1}, $k_5 = 10^6$ M^{-1} s^{-1} and $k_6 = 0$ s^{-1}. The initial rates of the increase in $\langle M \rangle_w$ in the second phase are 18.6, 10.0 and 5.4/s for $c_0 = 2.0$, 1.0 and 0.5×10^{-5} M respectively. These are approximately proportional to the second power of c_0 when multiplied by c_0 (the value corresponding to the turbidity). When $k_5 \approx 0$, there is no appreciable concentration dependence and these three curves agree closely within the line width.

the degree of polymerization when the transient-saturation occurs decreases with increasing protein concentration in fig. 4. This fact suggests that in an actual TMV-protein system the number of monomers composing the nucleus is greater than two [31].

Second, the existence of the inflection point in the second phase is not simulated. Discussions will be given about this point.

4. Discussion

4.1. The relation of the present result with the polymerization reaction of actin and that of myosin

Among the established mechanisms of the kinetics of the polymerization reaction of protein, theoretical studies by Oosawa and Kasai [26] and Oosawa [27], and experimental works by Kasai [28] and Kawamura and Maruyama [29] on the polymerization reaction of actin are closely related with the present work. Oosawa [27] showed that the polymerization reaction having the characteristics of crystallization consists of three stages; nucleation, growth, and redistribution of the polymer size. In the first and second stages, the concentration of monomers decreases and approaches closely the equilibrium value, $c_{1,eq.}$. If, a spontaneous nucleation is inhibited and the polymerization takes place by the addition of monomers to pre-existing seeds, a Poisson type peaked distribution is attained. In the third stage, the size distribution of polymers is slowly transformed into an exponential type in the same way as a diffusion process. The change of the type of the distribution of polymers in the polymerization process as predicted above was in fact observed experimentally by Kawamura and Maruyama by an electron microscopic study of the polymerization reaction of F-actin transformed from Mg-polymer [29]. It was also computer-simulated [30].

In the case of a spontaneous nucleation, an approximate formula for the time course of the change of the population of monomers participating in polymers, $F(t)$, has been given by Oosawa and Kasai when the polymerization reaction is irreversible [26]. It predicts that the time course profiles of $F(t)$ for various solvent conditions are similar; they can be superimposed, when normalized to the total protein concentration, by a translation parallel to the log-time axis. Thus, the change in the type of the polymerization profile does not exist, and this was indeed the case when the polymerization reaction of actin was induced at various KCl concentrations and at various temperatures [28].

In the present work, it was found that the time course profile of the turbidity increase became the transient-saturation type when a rapid environmental change was made to that corresponding to the extremely polymerizing conditions. The transient-saturation was also predicted to occur under the addition-polymerization scheme by the simulation study. The mechanisms causing this type of polymerization revealed in the present work are as follows. First, accompanying the large and rapid environmental change favoring polymerization, a large number of nuclei are formed relatively easily and more than at equilibrium. This leads both to the peaked distribution of short polymers and to the rapid reduction in the concentration of the monomers to the final equilibrium value. These two correspond to the rapid increase in the turbidity and its transient-saturation, respectively.

The absence of the transient-saturation in NBS-modified TMV-protein can be explained by its difficulty in the nucleation reaction. And this difficulty apparently correlates with the fact that this protein cannot make a disk structure in the neutral pH region. But the question of what is the nucleus in the polymerization reaction in the mild acid region has not been solved.

The first phase in the transient-saturation type polymerization has the same nature as that in Oosawa's theory. But, the second phase is different from the redistribution phase in Oosawa's theory. In the latter, a redistribution occurs through the depolymerization and repolymerization of the polymerizing unit at the end of polymers. As $k_4 \approx k_3 c_{1,eq.}$ at this stage, the number of polymers remains constant, and so does the number average degree of polymerization. In the present case, however, the first transient peak distribution is slowly shifted to the longer length side. The number average length of the polymers calculated from the distribution data in fig. 10 (a) is shifted from 600 Å at 20 s to 1250 Å at 10 min. The elongation of the polymers which are formed in the first phase by the addition of the unreacted free monomers cannot explain this shift, because the number of the free monomers at the end of the first phase, when estimated from the degree of agreement of the calculated turbidity value with the measured one (fig. 10 (a)), cannot be so great as to afford this shift.

These facts and the experimentally observed depen-

dence of the polymerization profile on the protein concentration can be explained by the assumption that polymer–polymer association reactions take place. If the polymer–polymer association reactions are considerably slow as compared with the monomer-addition reactions ($k_5 \ll k_3$), the transient-saturation occurs as well as when only the monomer-addition reactions take place. Short polymers which have been formed before the transient-saturation occurs associate with each other and longer polymers are produced slowly. Of course, no transient-saturation was observed in the simulation when the polymer–polymer association reactions took place with a rate comparable to that of the monomer-addition reaction ($k_5 \approx k_3$).

The existence of the inflection point in the second phase could not be explained by the scheme which includes the polymer–polymer association reactions. One possibility to explain this is to introduce two conformations in the polymer state. Assuming that the short polymers which have been formed before the transient-saturation occurs cannot associate with each other, but that they can associate after they perform a conformation change, the inflection was found to be simulated well. But this assumption, on the other hand, made the concentration dependence of the initial slope in the second phase weaker than the second order. Moreover, a temperature-jump circular dichroism measurement could not have detected such a conformation change. Thus, this problem remains to be solved.

After the polymer–polymer association phase, the distribution becomes broad. Though this broadening seems to have a similar nature as the redistribution process in Oosawa's theory, it was found that the distribution did not become an exponential type after two days.

The formation of a peaked distribution was through a spontaneous nucleation in the present work. Similar situations have been shown in the polymerization reaction of myosin [32,33]. The formation of myosin filaments was achieved spontaneously by lowering the KCl concentration (by dilution or dialysis). The pH and the ionic strength of the solution determined the size and the other features of myosin filaments. It is further known that the length distribution of filaments was dependent on the speed of the lowering of the KCl concentration [34,35]. When the filaments were made by a fast dilution (dilution time below one second), they were short (average length of about 0.5 μ) and comparatively uniform in length. On the other hand when they were made by a slow dilution (dilution time of several minutes), they were heterogeneous in length (from about 0.2 to 2.0 μ), and both short and long filaments were formed. These length distributions did not change, at least for two days.

The first point, the spontaneous peaked distribution formation of myosin under a rapid environmental change, is also seen in TMV-protein. But, in the present case, the first transient peaked distribution shifted to longer lengths and also broadened in the second phase. The second point, a heterogeneous distribution formation under a slow environmental change, is also seen in TMV-protein (fig. 8). Regarding this point, our recent finding is that under a temperature-jump from 4 to 16°C, very long polymers ($\approx$1 μ) are formed after several minutes. And the result in fig. 8 can be explained if this fact is also taken into consideration; i.e., under a slow temperature change from 4 to 25°C, long polymers are formed when the temperature of the solution is relatively low and as it increases, short polymers begins to be formed.

4.2. Transient-overshoot type polymerization

Scheele and Schuster reported that in the polymerization reaction of TMV-protein a transient-overshoot in the molecular weight occurred when the temperature of the solution was rapidly raised from 4 to 20°C at pH 6.5 [8]. By means of a computer simulation, they showed that if the polymerizing system involved a slow nucleation step and subsequent fast propagation steps, the latter steps would result in the population of longer polymers higher than at the equilibrium, and a transient-overshoot in the weight average degree of polymerization occurs.

We could not observe this effect by turbidimetry in the concentration range from 0.5 to 2.0 mg/ml. At present, the precise experimental conditions (the method of temperature change, that of measuring the extent of polymerization, or the concentration of the protein) in the study by Scheele and Schuster are not known, and a comparison with those of the present one cannot be made.

Recently Adiarte et al. showed that an overshoot type polymerization did occur in their stopped-flow experiment; the disk formation reaction after a pH-

jump from pH 8 to 6.9. In their experiment a transient-overshoot in the decrease of transmittance was observed when the concentration of the protein was higher than 3 mg/ml. Their results contrast with the present one shown in fig. 3 in two aspects; the extent of polymerization (much greater in the present case) and the profile of polymerization (transient-overshoot in their results and transient-saturation in the present work).

The first aspect has already been described in section 3.1.1. Regarding the second aspect the differences in the experimental conditions must be considered; the initial state of the protein (K-phosphate, pH 8, ionic strength 0.1, $T > 20°C$, and K/Na-phosphate, pH 6.9, ionic strength 0.1, $T = 11°C$), the composition of the buffer (K-phosphate plus 0.1 M KCl/0.006 N HCl, and K/Na-phosphate), the concentration of the protein, and the strain of TMV. The former two may be of minor importance. The latter two seem to be important. Especially, regarding the concentration, the results of the simulation by Scheele and Schuster show that no overshoot occurs when the initial monomer concentration is below a certain level. The clarification of this point will need further experiments on this line.

Acknowledgement

We wish to thank Drs. Y. Kiho and T. Hayashi of the Institute for Plant Virus Research for providing us the TMV-infected leaves for the present work, and Drs. Y. Okada and T. Ohno for various suggestions and discussions. We are indebted to Dr. T. Wakabayashi for help with various aspects of electron microscopy, and for kindly supplying us a grid of tropomyosin magnesium tactoids. We thank also Mrs. K. Sakurai for sedimentation velocity measurement. This work was partially supported by a Grant-in-Aid for Fundamental Scientific Research from the Ministry of Education of Japan.

Appendix

In this appendix, the relation used in section 3.1.3. is derived. The temporal changes of the molar concentration of monomers, c_1, and that of each polymer, c_i, in the monomer addition scheme are described as follows:

$$\begin{aligned}
dc_1/dt &= -k_1c_1(c_1+c_2+c_3+\ldots+c_{i_0-1}) + k_2(2c_2+c_3+\ldots+c_{i_0}) \\
&\quad - k_3c_1(c_{i_0}+c_{i_0+1}+\ldots+c_i+\ldots) + k_4(c_{i_0+1}+c_{i_0+2}+\ldots+c_i+\ldots) \\
dc_2/dt &= k_1c_1(c_1/2 - c_2) - k_2(c_2 - c_3) \\
dc_3/dt &= k_1c_1(c_2 - c_3) - k_2(c_3 - c_4) \\
dc_{i_0}/dt &= k_1c_1c_{i_0-1} - k_3c_1c_{i_0} - k_2c_{i_0} + k_4c_{i_0+1} \\
dc_{i_0+1}/dt &= k_3c_1(c_{i_0} - c_{i_0+1}) - k_4(c_{i_0+1} - c_{i_0+2}) \\
dc_i/dt &= k_3c_1(c_{i-1} - c_i) - k_4(c_i - c_{i+1}) .
\end{aligned} \tag{1}$$

Here, the nucleus is assumed to consist of i_0 monomers, and the limit of the polymer length is not assumed.

For simplicity, we put $k_1 = k_3$, and $k_2 = k_4$. Then the temporal change of the weight average degree of polymerization, $\langle i\rangle_w$, is calculated as follows:

$$\begin{aligned}
\frac{d\langle i\rangle_w}{dt} &= \frac{d(\sum i^2c_i/\sum ic_i)}{dt} = \frac{d(\sum i^2c_i/c_0)}{dt} \\
&= \frac{d(\sum i(i-1)c_i/c_0)}{dt} + \frac{d(\sum ic_i/c_0)}{dt} \\
&= \frac{d(\sum i(i-1)c_i/c_0)}{dt} = \sum \frac{i(i-1)(dc_i/dt)}{c_0} .
\end{aligned} \tag{2}$$

Here, $c_0 = \Sigma ic_i$ is the total concentration. Substituting (1) into (2) and after some rearrangement the final formula

$$d\langle i\rangle_w/dt = k_1c_1(2 - c_1/c_0) - 2k_2(1 - \sum_1^\infty c_i/c_0)$$

is obtained.

We consider the initial rate of the turbidity decrease when the environmental condition of the polymer solution is rapidly changed to that favoring depolymerization; $k_1c_1 \ll k_2$. If in the initial state only polymers are present, and the number average degree of polymerization, $\langle i\rangle_n = \Sigma ic_i/\Sigma c_i = c_0/\Sigma c_i$, is high enough, then, $d\langle i\rangle_w/dt = -2k_2$ at $t = 0$. Turbidity, τ, is given by $Hc\langle M\rangle_w$, where H is the optical constant, c is the concentration of proteins in g/ml,

and $\langle M \rangle_w$ is the weight average molecular weight. Thus, the relation $d\tau/dt = HcM_0 d\langle i \rangle_w/dt = -2k_2\tau_0$ is obtained, where M_0 is the molecular weight of the monomer, and τ_0 is the turbidity of the monomer solution. In the case when $k_1 \neq k_3$ and $k_2 \neq k_4$, the relation $d\tau/dt = -2k_4\tau_0$ for the initial rate is obtained, if c_i's ($i \leqslant i_0$) are negligible, and this relation is used in the text.

References

[1] H. Fraenkel-Conrat and R.C. Williams, Proc. Natl. Acad. Sci. (U.S.) 41 (1955) 690.
[2] G. Schramm and W. Zillig, Z. Naturforsch. 10b (1955) 493.
[3] M.A. Lauffer, A.T. Ansevin, T.E. Cartwright and C.C. Brinton, Jr., Nature 181 (1958) 1338.
[4] For reviews, see M.A. Lauffer and C.L. Stevens, Adv. Virus Res. 13 (1968) 1, or M.A. Lauffer, in: Subunits in Biological Systems, Part A, eds. S.N. Timasheff and D. Fasman (Marcel Dekker, Inc., New York, 1971) p. 149.
[5] A.T. Ansevin and M.A. Lauffer, Biophys. J. 3 (1963) 239.
[6] A.C.H. Durham and A. Klug, Nature New Biol. 229 (1971) 42.
[7] A.C.H. Durham, J. Mol. Biol. 67 (1972) 289.
[8] R.B. Scheele and T.M. Schuster, Biopolymers 13 (1974) 275.
[9] A.L. Adiarte, D. Vogel and R. Jaenicke, Biochem. Biophys. Res. Commun. 63 (1975) 432.
[10] F.M. Pohl, Eur. J. Biochem. 4 (1968) 373.
[11] S. Segawa, Y. Husimi and A. Wada, Biopolymers 12 (1973) 2521.
[12] H. Boedker and N.S. Simmons, J. Am. Chem. Soc. 80 (1958) 2550.
[13] H. Fraenkel-Conrat, Virology 4 (1957) 1.
[14] T. Ohno, R. Yamaura, K. Kuriyama, H. Inoue and Y. Okada, Virology 50 (1972) 76.
[15] H. Inoue, K. Kuriyama, T. Ohno and Y. Okada, Arch. Biochem. Biophys. 165 (1974) 34.
[16] P. Doty and R.F. Steiner, J. Chem. Phys. 18 (1950) 1211.
[17] D.L.D. Caspar, C. Cohen and W. Longley, J. Mol. Biol. 41 (1969) 87.
[18] A.C.H. Durham and J.T. Finch, J. Mol. Biol. 67 (1972) 307.
[19] C.E. Smith and M.A. Lauffer, Biochemistry 6 (1967) 2457.
[20] P. Henrici, Discrete Variable Methods in Differential Equations (Wiley, New York, 1962).
[21] A.F. Shalaby and M.A. Lauffer, Biochemistry 6 (1967) 2465.
[22] Y. Nozu and Y. Okada, J. Mol. Biol. 35 (1968) 643.
[23] F. Gaskin, C.R. Cantor and M. Shelanski, J. Mol. Biol. 89 (1974) 737.
[24] C.E. Hall, Introduction to Electron Microscopy, 2nd ed. (McGraw-Hill, New York, 1966) p. 358.
[25] A. Wegner and J. Engel, Biophys. Chem. 3 (1975) 215.
[26] F. Oosawa and M. Kasai, J. Mol. Biol. 4 (1962) 10.
[27] F. Oosawa, J. Theor. Biol. 27 (1970) 69.
[28] M. Kasai, Biochim. Biophys. Acta 180 (1969) 399.
[29] M. Kawamura and K. Maruyama, Biochim. Biophys. Acta 267 (1972) 422.
[30] F. Arisaka, M. Kawamura and K. Maruyama, J. Biochem. (Tokyo) 73 (1973) 1211.
[31] K. Wakabayashi, H. Hotani and S. Asakura, Biochim. Biophys. Acta 175 (1969) 195.
[32] B. Kaminer and A.L. Bell, J. Mol. Biol. 20 (1966) 391.
[33] R. Josephs and W.F. Harrington, Biochemistry 5 (1966) 3474.
[34] K. Takahashi, Protein Nucleic Acid Enzyme (in Japanese) 12 (1967) 61.
[35] I. Katsura and H. Noda, J. Biochem. (Tokyo) 69 (1971) 219.